J Solid State Electrochem (2010) 14:2077–2082
DOI 10.1007/s10008-010-1018-8

ORIGINAL PAPER

Electro-catalytic performance of PdCo bimetallic hollow nano-spheres for the oxidation of formic acid

Yawen Tang · Yu Chen · Ping Zhou · Yiming Zhou · Lude Lu · Jianchun Bao · Tianhong Lu

Received: 14 October 2009 / Revised: 18 January 2010 / Accepted: 27 January 2010 / Published online: 24 March 2010

Abstract PdCo bimetallic hollow nano-spheres anodic catalyst has been synthesized through a simple simultaneous reduction reaction using polyglycol as template. The images of transmission electron microscopy show that the average diameter of the PdCo hollow nano-spheres is about 80 nm and the shell thickness is about 9.0 nm. The electrochemical measurements indicate that the electro-catalytic activity and stability of PdCo hollow nano-spheres catalyst for formic acid oxidation is much better than that of the PdCo solid nano-spheres and Pd solid nano-spheres, which is ascribed to the unusual chemical and physical properties of the PdCo hollow nano-spheres, such as the interior micro/nano structure, the particular electronic property, and the promotion of the direct dehydrogenation path of formic acid oxidation.

Keywords Fuel cell · PdCo hollow nano-spheres · Catalyst · Formic acid · Oxidation

Introduction

Direct formic acid fuel cells (DFAFCs) has attracted more and more attention as a new generation of environment-friendly power source with high operating power densities, which is particularly suitable for portable devices such as cellular phones, personal digital assistants, laptop computers, etc. [1–10]. The success of the DFAFCs largely depends on the design and preparation of high performance anode catalysts. Recent investigations have suggested that Pd catalyst possesses better electro-catalytic activity for the formic acid oxidation than Pt catalyst, but loses easily a large amount of its activity during formic acid oxidation owing to either the oxidation of Pd surfaces or the poisoning adsorption of CO_{ads} species [1]. Thus, a lot of effort has been devoted to improving the electro-catalytic activity and stability of Pd catalyst, which is achieved by reducing Pd particle size, changing Pd particle morphology, and constructing Pd-based alloy catalysts [1–10].

It is well-known that the electro-catalytic activity of Pt-based and Pd-based catalysts strongly depends on the size, electronic, structural, and geometric properties of metal nano-particles in catalyst. Although the hollow nanostructure metal materials, one of the important material structures, is especially attractive for catalytic action due to its unusual chemical and physical characteristics such as interior micro/nano structure, low density, and large surface area [11–13], the application of precious metals' hollow nano-spheres materials in low temperature fuel cell is rare [12, 13]. To our knowledge, there is no such report on the application of Pd-based hollow nano-spheres in DFAFCs.

In this paper, a simple simultaneous reduction reaction method has been used to prepare the PdCo bimetallic hollow nano-spheres by using polyglycol as template. The morphology and structure of the PdCo bimetallic hollow nano-spheres were characterized by transmission electron microscopy (TEM), scan electron microscopy (SEM), energy dispersive spectrometer (EDS), X-ray diffraction (XRD), and X-ray photoelectron spectroscopy (XPS) measurements. Meanwhile, the electro-catalytic properties of the PdCo bimetallic

Y. Tang · L. Lu · J. Bao
Materials Chemistry Laboratory,
Nanjing University of Science and Technology,
Nanjing 210094, People's Republic of China

Y. Tang · Y. Chen · P. Zhou · Y. Zhou · J. Bao · T. Lu (✉)
College of Chemistry and Environmental Science,
Nanjing Normal University,
Nanjing 210097, People's Republic of China
e-mail: tianhonglu@263.net

hollow nano-spheres anodic catalyst for formic acid oxidation were also investigated by typical electrochemical methods.

Experimental

Preparation of catalysts

All chemical reagents were analytical grade and were obtained from Shanghai Chemical Regent Ltd. The PdCo hollow nano-spheres were prepared as follows: 42 mg $CoSO_4 \cdot 7H_2O$, 25 mg NH_4F, 125 mg H_3BO_3, and 24 mg H_2PdCl_4 were added into 10 mL 0.25 g mL^{-1} polyglycol (M_w 20,000) solution. After the pH of the solution was adjusted to 7–8 using concentrated ammonia, the appropriate amounts of $NaBH_4$ solution was added to the solution under sonication conditions at 30–40 °C. After the precipitate was washed and dried, the PdCo bimetallic hollow nano-spheres catalyst was obtained and was noted as PdCo–H catalyst. For comparison, the PdCo catalyst with the solid sphere structure was also prepared. The preparation method is similar to that of the PdCo–H catalyst except that polyglycol was not added. The catalyst prepared was noted as the PdCo–S catalyst. When $CoSO_4$ was not added, the Pd solid nano-spheres catalyst obtained was noted as the Pd–S catalyst.

Physicochemical and electrochemical measurements

The morphology and particle sizes of the PdCo hollow spheres were measured with JEM-200CX TEM and SSX550 SEM. The composition of catalysts was determined using the EDS with Vantage Digital Acquisition Engine. The XRD pattern of the PdCo hollow nano-spheres was obtained using a Rigaku-D/MAX-PC 2500 X-ray diffractometer. XPS measurements were carried out on a Kratos XSAM-800 spectrometer. Detailed Pd3d and Co2p signals were collected and analyzed. The electrochemical measurements were performed in a conventional three-electrode electrochemical cell by using a CHI 600 electrochemical analyzer at 30±2 °C. A Pt plate and a saturated calomel electrode (SCE) were used as the auxiliary electrode and the reference electrode, respectively. All potentials were quoted with respect to SCE. The working electrode was prepared according to the literature procedure [14]. The loading of Pd on the electrode surface was 28 μg cm^{-2}.

Results and discussion

Physicochemical characterization of catalysts

Figure 1a shows the TEM image of the PdCo hollow nano-spheres (i.e., PdCo–H catalyst). In each sphere, the central part has the pale color and the edge part shows the dark color. There is no obvious change between the center and edge of the spheres when the sample grid is rotated by different degrees, illustrating that the PdCo–H catalyst possesses the structure of the hollow sphere. It is observed that the average particle diameter of the PdCo–H catalyst is about 80 nm, mainly ranging from 60 to 90 nm, which is coincident with experimental result of the scanning electron micrograph (SEM) in Fig. 1b. Meanwhile, it is also observed from Fig. 1a that the shell thickness of the PdCo–H catalyst is about 9 nm. In addition, the crystalline feature of PdCo hollow nano-spheres is explored by a selected area electron diffraction (SAED) pattern (inset in Fig. 1a). The SAED reveals that PdCo hollow nano-spheres have face centered cubic (fcc) structure corresponding to (111), (200), (220), (311), and (420) Pd crystalline facets, showing that PdCo hollow nano-spheres include many small particles that have independent orientations.

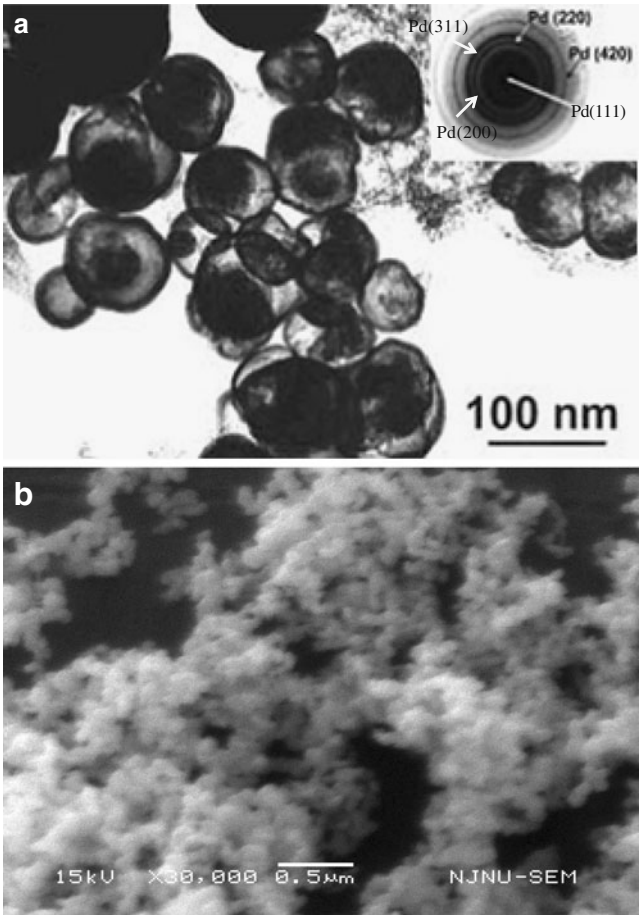

Fig. 1 TEM image (**a**) and SEM pattern (**b**) of the PdCo–H catalyst. *Inset* (**a**) indicates electron diffraction pattern of PdCo–H catalyst

Figure 2 A shows the EDS spectrum of the PdCo–H catalyst. The EDS measurement indicates that the atomic ratio of Pd and Co in the PdCo–H catalyst is 3.5:1. The EDS spectrum of the PdCo–S catalyst is similar to that of

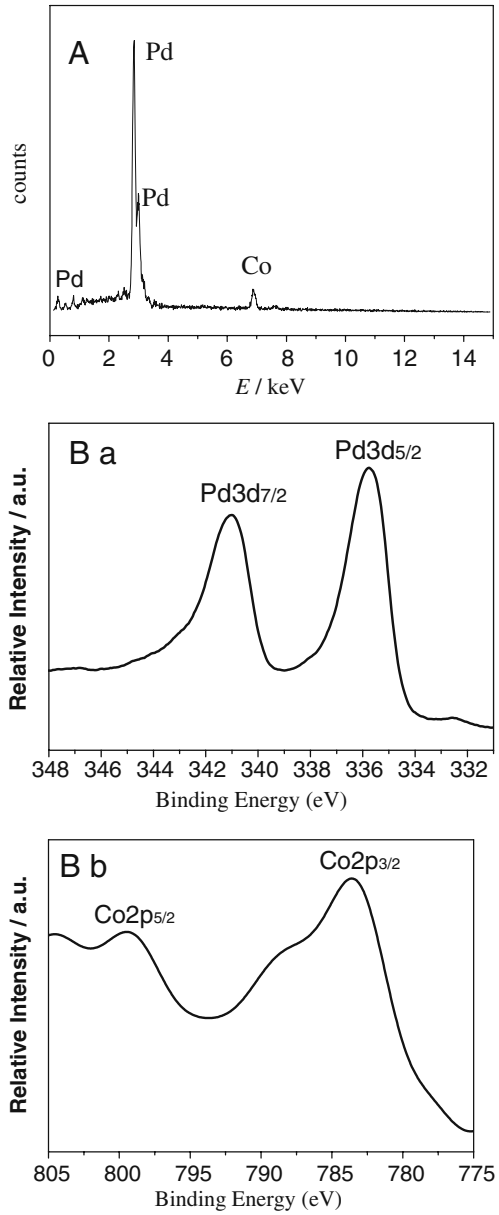

Fig. 2 *A* EDS spectrum of the PdCo–H catalyst; *B* XPS spectra of PdCo–H catalyst in the *a* Pd3d and *b* Co2p region

the PdCo–H catalyst and the atomic ratio of Pd and Co in the Pd–Co–S catalyst is also near 3.5:1 (data not shown). The surface composition of the PdCo–H catalyst is further investigated by XPS measurement. As shown in Fig. 2 B, the binding energies of $Pd3d_{5/2}$ and $Pd3d_{3/2}$ of PdCo–H catalyst are 335.8 and 341.0 eV, respectively, which are 0.7 eV higher than that of 40-nm solid Pd nano-spheres in the literature [15]. The shift of binding energy may be attributed to size effect of nanoparticle [6, 15] and/or interaction between Pd with Co atoms, which can result in a decrease of the 3d electron density of Pd atom in PdCo–H catalyst. Meanwhile, it is observed that there is a small chemical shift toward higher binding energies for $Co2p_{3/2}$ (783.3 eV) and $Co2p_{1/2}$ (799.2 eV) as compared to metallic Co [16], implying that the partial Co in the PdCo–H catalyst is the oxidation state.

To further obtain the crystallographic information of PdCo–H catalyst, an XRD measurement was conducted. As shown in Fig. 3a, three diffraction peaks of PdCo hollow nano-spheres located at 40.28°, 46.75°, and 68.39°, corresponding to the characteristic diffraction peak of the face centered cubic crystalline of pure Pd, respectively [ASTM standard 5-681 (Pd)]. Similarly, three characteristic peaks of pure Pd are also observed in the XRD patterns of PdCo–S (Fig. 3b) and Pd–S (Fig. 3c) catalysts, respectively. Compared to Pd–S catalyst (Fig. 3c), the diffraction peaks of PdCo–H and PdCo–S catalysts are shifted to higher 2θ value. Meanwhile, no obvious peaks related to Co are observed in both PdCo–H and PdCo–S catalysts. Thus, the positive shift of the diffraction peaks in PdCo–H and PdCo–S catalyst indicates that Co atoms have entered into the crystal lattice of Pd, forming the PdCo alloy. The average particles sizes of three catalysts were calculated using Debye–Scherrer formula [17]. The average sizes of the particles in the PdCo–S and Pd–S catalysts are calculated to be 38 and 27 nm, respectively, which are consistent with the results of TEM measurements (Fig. 4). However, the average particle size from the XRD patterns is 4.1 nm for PdCo–H catalyst, which is much smaller than average particle size from the TEM measurement. The fact demonstrates that the PdCo–H hollow nano-spheres catalyst is composed of small primary crystals PdCo nano-particles with a size of 4.1 nm [18]. Thus, the PdCo hollow nano-spheres can afford more active site for reactant in the course of catalytic action due to the particular interior micro/nano structure.

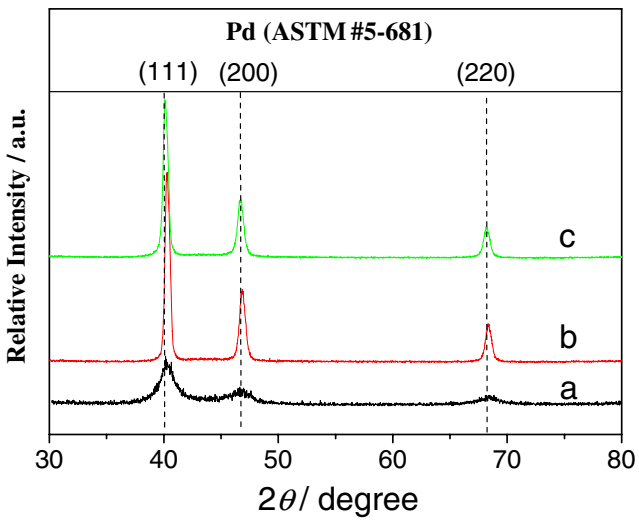

Fig. 3 XRD patterns of the PdCo–H (**a**), PdCo–S (**b**), and Pd–S (**c**) catalysts

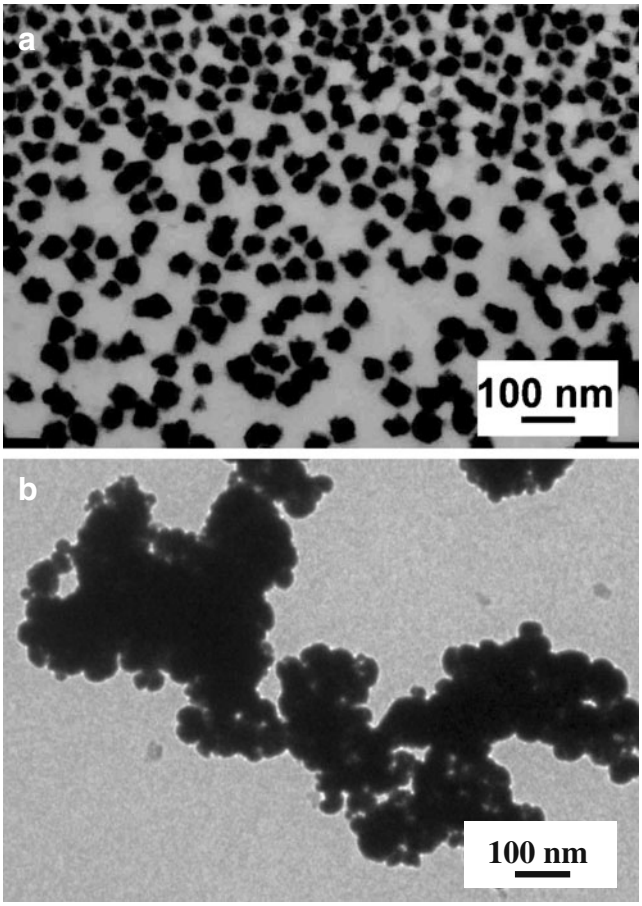

Fig. 4 TEM images of the PdCo–S (**a**) and Pd–S (**b**) catalysts

It is necessary to point out that PdCo hollow nanospheres can be easily obtained in high yields up to 70% by using the present method. When the PdCo catalyst is prepared in the absence of polyglycol, only the solid PdCo particles with 40-nm average size can be obtained, and they are uniformly distributed (Fig. 4a). In addition, if the catalyst is prepared in the absence of $CoSO_4$, the Pd hollow spheres can't be obtained. Herein, only the Pd solid particles with the 30 nm average size are obtained and they are significantly aggregated (Fig. 4b), illustrating that Co^{2+} ion plays the important role for the formation of the hollow spheres and uniform distribution of particles. We speculate that the formation of the PdCo hollow spheres might result from polyethylene glycol spherical aggregates formed mainly via the affinity of the oxygen atoms of the polyethylene glycol for Co^{2+} ions. In such aggregates, the hydrophobic hydrocarbon chains of the polyethylene glycol are oriented toward the interior of the aggregates, while the $[PdCl_4]^{2-}$ and Co^{2+} ions are mainly located on the surface of the aggregates to form a Co- and Pd-containing coating which creates a nucleation domain of Co and Pd for the subsequent redox reaction.

Cyclic voltammetric characteristics of catalysts

Hydrogen adsorption and absorption peaks at Pd surfaces provide important information about surface structure of Pd-based catalysts. Figure 5 presents the cyclic voltammograms of the PdCo–H, PdCo–S, and Pd–S catalysts in the 0.5 M H_2SO_4 solution. In the hydrogen adsorption/desorption region (−0.2–0.05 V), the coulomb charge for hydrogen desorption was used to calculate the electrochemically active surface (EAS) of catalysts [19, 20]. The EAS of the PdCo–H, PdCo–S, and Pd–S catalyst are 12.9, 5.0, and 5.8 $m^2\ g^{-1}$, respectively. This result indicates that EAS of the PdCo hollow spheres is higher than that of the PdCo–S and Pd–S catalysts. It may be due to the interior hollow structure of PdCo–H catalyst, which results in a larger specific surface area, compared with that of PdCo–S and Pd–S catalysts.

Formic acid electro-oxidation

Figure 6 displays the cyclic voltammograms of 0.5 M HCOOH in the 0.5 M H_2SO_4 solution at the PdCo–H, PdCo–S, and Pd–S catalyst. In the positive scan direction, the two oxidative peaks of formic acid are located at 0.10 V and 0.54 V for all electrodes, which correspond with the two pathways of the formic acid oxidation, i.e., the direct pathway and the CO pathway [21]. This result indicates that the existence of Co does not affect obviously the peak potential of the formic acid oxidation at the Pd catalyst. Although PdCo–H catalyst possesses larger diameter (Fig. 1) than that of PdCo–S and Pd–S catalysts (Fig. 4), the oxidation current of formic acid at 0.1 V for the PdCo–H, PdCo–S, and Pd–S catalysts are 180.2, 57.4, and 50.6 mA mg^{-1} (Pd), respectively. This illustrated that the mass electrocatalytic activity of the PdCo–H catalyst for the formic acid

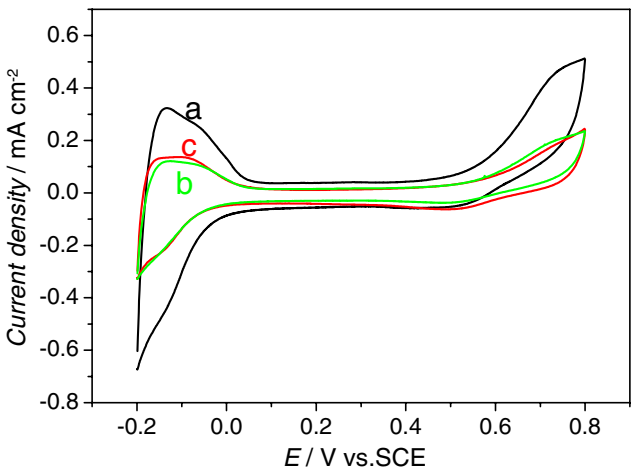

Fig. 5 Cyclic voltammograms of the PdCo–H (**a**), PdCo–S (**b**), and Pd–S (**c**) catalysts in the 0.5 M H_2SO_4 solution at the scan rate of 50 mV s^{-1}

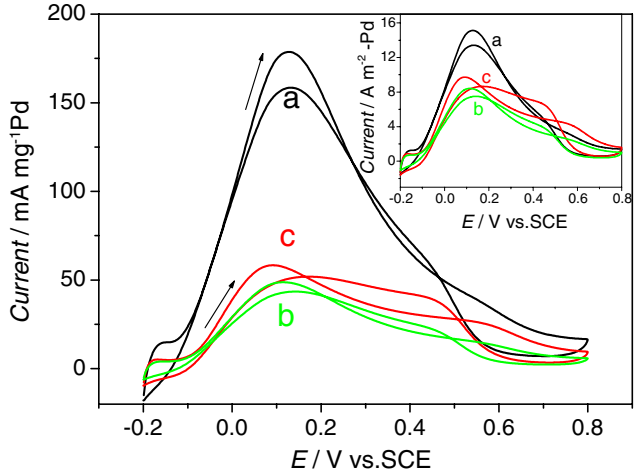

Fig. 6 Cyclic voltammograms of 0.5 M HCOOH in 0.5 M H_2SO_4 solution at the PdCo–H (**a**), PdCo–S (**b**), and Pd–S (**c**) catalysts at the scan rate of 50 mV s^{-1}. The inset shows the CVs normalized using the Pd surface area (mA m^{-2} Pd)

electro-oxidation is much better than that of the PdCo–S and Pd–S catalysts. Moreover, we also normalized the oxidation current of formic acid by using the Pd electrochemically active surface area and plotted the CV curves (inset) for comparison with the curves normalized using the mass activity of catalysts (Fig. 6) [22]. Obviously, it is observed from the inset that the PdCo–H catalyst exhibits a bigger oxidation current of formic acid at 0.1 V than PdCo–S and Pd–S catalysts. The results of specific activity measurements show that the intrinsic electro-activity of PdCo–H catalyst is much better than that of PdCo–S and Pd–S catalysts. In addition, it is observed that the ratio of the peak current at 0.1 and 0.5 V at the PdCo–H catalyst is obviously much larger than that at the PdCo–S and Pd–S catalysts. This illustrates that the extent of the formic acid oxidation via the direct pathway at the PdCo–H catalyst is obviously much larger than that at the PdCo–S and Pd–S catalysts. Very possibly, the lower 3d electron density of Pd atom in PdCo–H catalyst (Fig. 2 B) results in a decrease in adsorption energy of the formate intermediate that enhances the rate of the formic acid oxidation via the direct path [15]. The improvement of electro-catalytic activity of the PdCo–H catalyst for the formic acid oxidation may be attributed to three major factors: (1) the EAS of the PdCo–H catalyst is bigger than that of the PdCo–S and Pd–S catalysts due to its particular hollow structure, which can afford more active site for the formic acid oxidation, (2) the PdCo hollow nano-spheres composed of small PdCo nano-particles possess a rough surface rather than a smooth one, which results in the presence of relatively high density of defects; such defects may have high activity as catalysts and provide more bonding sites for the formic acid oxidation [13], (3) the particular electronic property of Pd atom in PdCo–H catalyst enhances the rate of the formic acid oxidation via the direct path [15].

The stability of Pd-based catalysts is extremely important for their real applications in DFAFCs. The activity and durability of the Pd-based catalysts are further assessed by chronoamperometry test. Figure 7 displays the chronoamperometric curves of 0.5 M HCOOH at the Pd–Co–H, Pd–Co–S, and Pd–S catalyst electrodes at 0.1 V. It is observed that the oxidation current of formic acid at the PdCo–H, PdCo–S, and Pd–S catalysts at 1,000 s are 64.8, 5.7, and 5.5 mA mg^{-1} (Pd), respectively, indicating that the electro-catalytic stability of the PdCo–H catalyst for the formic acid oxidation is better than that of the PdCo–S, Pd–S catalysts, and reported Pd/C catalyst (53.8 mA mg^{-1} (Pd)) in the ref. [20]. As mentioned above, most of formic acid is oxidized through the direct pathway at the PdCo–H catalyst electrode. Therefore, the PdCo–H catalyst electrode is not easy to be poisoned with CO. As a result, the electro-catalytic stability of the PdCo–H catalyst for the formic acid oxidation is very excellent.

Conclusions

In summary, a facile procedure for the synthesis of PdCo bimetallic hollow nano-spheres was developed. Comparing with the PdCo solid spheres and Pd solid spheres catalysts, PdCo hollow nano-spheres catalyst improve obviously the electro-catalytic activity and stability for formic acid oxidation. This is ascribed to its unusual chemical and physical properties, such as the interior micro/nano structure, the particular electronic property, the large surface area, and the promotion of formic acid oxidation via the direct dehydrogenation path. The PdCo bimetallic hollow nano-spheres catalyst can be useful in industrial applications including DFAFCs and related fields.

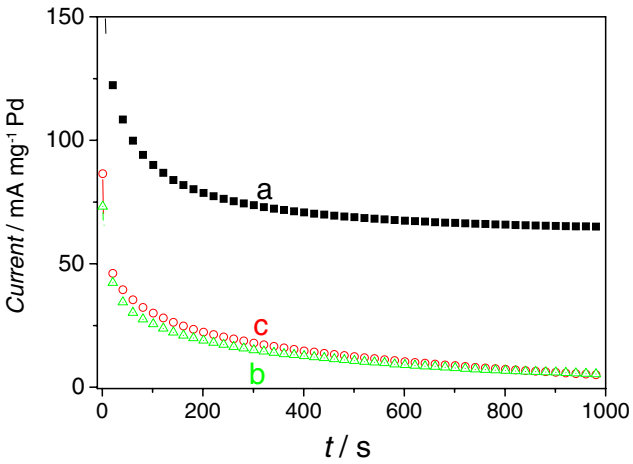

Fig. 7 Chronoamperometric curves of 0.5 M HCOOH in the 0.5 M H_2SO_4 solution at the PdCo–H (**a**), PdCo–S (**b**), and Pd–S (**c**) catalysts at the 0.1 V fixed potential

Acknowledgment The authors are grateful for the financial support of State Key High Technology Research Program of China (863 Program, 2006AA05Z137, 2007AA05Z143, 2007AA05Z159) of Science and Technology Ministry of China, the National Natural Science Foundation of China (20873065).

References

1. Wang JY, Kang YY, Yang H, Cai WB (2009) J Phys Chem C 113:8366
2. Liao C, Wei ZD, Chen SG, Li L, Ji MB, Tan Y, Liao MJ (2009) J Phys Chem C 113:5705
3. Mazumder V, Sun SH (2009) J Am Chem Soc 131:4588
4. Meng H, Sun SH, Masse JP, Dodelet JD (2008) Chem Mater 20:6998
5. Lee H, Habas SE, Somorjai GA, Yang PD (2008) J Am Chem Soc 130:5406
6. Zhou WJ, Lee JY (2008) J Phys Chem C 112:3789
7. Haan JL, Masel RI (2009) Electrochimica Acta 54:4073
8. Zhua Y, Khana Z (2005) J Power Sources 139:15
9. Li X, Hsing IM (2006) Electrochimica Acta 51:3477
10. Ha S, Larsen R, Masel RI (2005) J Power Sources 144:28
11. Chen G, Xia D, Nie Z, Wang Z, Wang L, Zhang L, Zhang J (2007) Chem Mater 19:1840
12. Zhao Y, Cai Y, Tian J, Lan H (2009) Mater Chem Phys 115:831
13. Chen H, Liu RS, Lo MY, Chang SC, Tsai LD, Peng YM, Lee JF (2008) J Phys Chem C 112:7522
14. Schmidt TJ, Gasteiger HA, Behm RJ (1999) J Electrochem Soc 146:1296
15. Zhou WP, Lewera A, Larsen R, Masel RI, Bagus PS, Wieckowski A (2006) J Phys Chem B 110:13393
16. Kastle G, Boyen HG, Weigl F, Lengl G, Herzog T, Ziemann P, Riethmuller S, Mayer O, Hartmann C, Spatz JP, Moller M, Ozawa M, Banhart F, Garnier MG, Oelhafen P (2003) Adv Funct Mater 13:853
17. Wang XM, Xia YY (2008) Electrochem Commun 10:1644
18. Ge JP, Hu YX, Biasini M, Beyermann WP, Yin YD (2007) Angew Chem Int Ed 46:4342
19. Pozio A, Francesco MD, Cemmi A, Cardellini F, Giorgi L (2002) J Power Sources 105:13
20. Zhang L, Tang Y, Bao J, Lu T, Li C (2006) J Power Sources 62:177
21. Wesselmark M, Lagergren C, Lindbergh G (2008) J Appl Electrochem 38:17
22. Larsen R, Ha S, Zakzeski J, Masel RI (2006) J Power Sources 157:78